Available online at www.sciencedirect.com

ScienceDirect

Procedia CIRP 58 (2017) 13 – 18

www.elsevier.com/locate/procedia

16th CIRP Conference on Modelling of Machining Operations

The influence the uncut chip thickness has on the stagnation point in orthogonal cutting

Mathias Agmell*, Daniel Johansson, Sampsa VA Laakso, Aylin Ahadi, Jan-Eric Ståhl

Lund University, Department of Mechanical Engineering, Box 118, 221 00 Lund, Sweden

* Corresponding author. Tel.: +46462221564. *E-mail address:* mathias.agmell@iprod.lth.se

Abstract

The effect of cutting data on the stagnation zone of a machining operation is of great interest since it governs the material flow around the cutting edge. The material flow has a significant influence on the mechanical properties of the machined surface. This paper presents a numerical model that is able to determine the effect that the uncut chip thickness has on the stagnation zone and the connection between the stagnation zone and the deformation layer in the machined subsurface.

Keywords: Machining; Finite element method (FEM); Stainless steel; Stagnation zone; Subsurface deformation

1. Introduction

The AISI 316L alloy is used for a wide range of industrial applications where steels of type AISI 304/304L have insufficient corrosion resistance. Typical examples are: machined parts for tube fittings, valves, components for pumps and heat exchangers. It is also a commonly used alloy in production of pharmaceuticals and foods. A machining operation causes a subsurface deformation in the machined surface, insight on the surface integrity of the workpiece is essential to predict the life time of the produced part. The subsurface deformation can have a drastic effect on the performance, such as corrosion, wear and fatigue resistance of the machined product [1,2]. In [3] it has been investigated how the stagnation point affects the residual stresses of the machined surface. In the studies presented in [4–6] the effect micro geometry of the insert and cutting speed has on the stagnation zone has been investigated. The aim of this paper is to investigate how the material flow at the stagnation zone is affected by the uncut chip thickness, which in turn will have an impact on the subsurface deformation of the workpiece.

Nomenclature

A	Johnson-Cook yield coefficient
a_p	Depth of cut
B	Johnson-Cook strain hardening coefficient
C	Johnson-Cook strain rate hardening coefficient
C_p	Specific heat capacity
E	Young's modulus
F_c	Primary cutting force
F_f	Feed force
h	Heat transfer coefficient
h_1	Uncut chip thickness
k	Thermal conductivity
n	Johnson-Cook strain hardening exponent
m	Johnson-Cook thermal softening exponent
P	Location of the stagnation point
q	Heat flux per unit of area
r_β	Edge radius
S	Separation location from machined surface and tool
T	Temperature
T_m	Melting temperature
T_X	Surface temperature in point X
T_Y	Surface temperature in point Y

doi:10.1016/j.procir.2017.03.183

T_0	Bulk temperature
v_c	Cutting speed
x	Ploughed depth
α	Clearance angle
α_T	Thermal expansion
γ	Rake angle
ε	Strain
$\dot{\varepsilon}$	Strain rate
$\dot{\varepsilon}_0$	Reference strain rate
θ	Stagnation angle
κ	Major cutting angle
μ	Coulomb friction coefficient
ρ	Density
σ	Flow stress
σ_n	Surface normal stress
τ_f	Frictional stress
τ_y	Shear strength

2. Machining mechanics and theoretical aspects

This part of the paper covers the theoretical aspects of the machining process that will be investigated by the numerical simulations.

2.1. Material flow

In a cutting process, a stagnation zone is formed at the interface between the cutting tool and the workpiece. Since the material flow in the workpiece must either move towards the rake face of the cutting tool and form the chip or be ploughed under the cutting tool and turn into the machined surface. Fig. 1 illustrates the material flow in the workpiece in a cutting operation. Point *P* is the location of the stagnation point. Point *S* is the location where the machined surface separates from the tool. The ploughed depth *x* is a small fraction of the uncut chip thickness h_1. The line *PU* represents the shear plane. The vectors $\overrightarrow{OS}$ and $\overrightarrow{OP}$ has a length equal to the edge radius r_β. The stagnation angle θ, is given by the angle between the vectors $\overrightarrow{OS}$ and $\overrightarrow{OP}$ as given in Eq. 1.

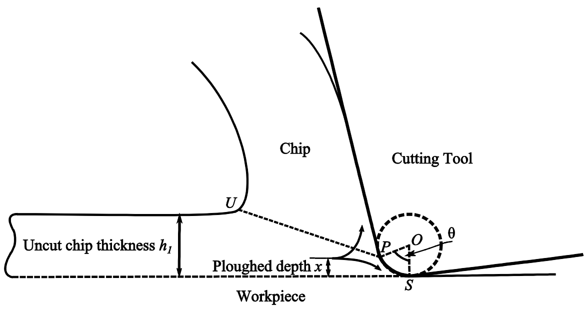

Fig. 1. Schematic view of the material flow.

$$\cos\theta = \frac{\left\langle \overrightarrow{OS}, \overrightarrow{OP} \right\rangle}{\| \overrightarrow{OS} \| \cdot \| \overrightarrow{OP} \|} \quad (1)$$

2.2. Stagnation Zone

Around point *P*, a stagnation zone will form where the material flow velocity of the workpiece will drastically decrease; thus, the shear stresses on the cutting tool will be close to zero in this region. The shear force component acting on the cutting tool, will change direction in the center of the stagnation zone at point *P*, illustrated by Fig. 2.

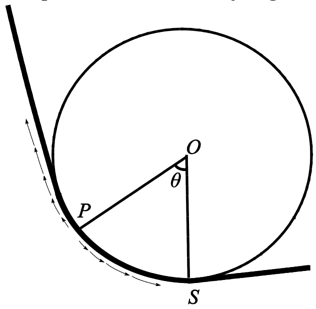

Fig. 2. Schematic view of the shear forces acting on the cutting tool at the stagnation zone.

3. Experimental investigation

As part of this investigation, experiments were performed through longitudinal turning of AISI 316L, with dry cutting conditions in a SMT 500 SWEDTURN CNC lathe. The tubes had an initial outer diameter of 80 mm and an inner diameter of 55 mm. The inserts used were industry standard cemented carbide inserts, SECO TOOLS CNMG120408-MF4 TM2000, with an edge radius r_β of approximately 45±5 µm. These inserts were mounted in a DCLNL 3225P12 tool holder with a major cutting angle κ=95° for all machining experiments. The cutting forces was measured with a cutting force sensor of the fabricate Kistler Z15814. The same cutting data was used for all the experiments; cutting speed v_c=125 m/min, while varying the feed in the steps 0.1 mm rev^{-1}, 0.2 mm rev^{-1}, 0.3 mm rev^{-1} and depth of cut a_p= 2 mm.

4. Numerical Modelling

4.1. FE-Formulation

The updated-Lagrangian formulation has been used for this analysis. Since Abaqus does not have a feature that automatically update the mesh, it has been performed with an implemented in-house Python script. The data transfer between the old and updated mesh has been achieved with the function *MAP SOLUTION. Fig. 3 shows a flow chart of the remeshing algorithm.

4.2. Material Modelling

The thermo-mechanical properties of both the tool and the workpiece are presented in Table 1. The temperature dependence of Young’s modulus, specific heat capacity and thermal conductivity for the workpiece has been considered and is presented in Table 2. To model the flow stress of AISI 316L the Johnson-Cook plasticity model was used, Eq. 2.